

# Degradation of Carbon Fiber-reinforced Epoxy Composites by Ultraviolet Radiation and Condensation

BHAVESH G. KUMAR, RAMAN P. SINGH\* AND TOSHIO NAKAMURA

*Department of Mechanical Engineering  
State University of New York  
Stony Brook, NY 11794, USA*

(Received December 13, 2001)  
(Revised June 14, 2002)

**ABSTRACT:** The degradation of an IM7/997 carbon fiber-reinforced epoxy exposed to ultraviolet radiation and/or condensation has been characterized. Based on observations of physical and chemical degradation it has been established that these environments operate in a synergistic manner that causes extensive erosion of the epoxy matrix, resulting in a reduction in mechanical properties. Matrix dominated properties are affected the most, with the transverse tensile strength decreasing by 29% after only 1000h of cyclic exposure to UV radiation and condensation. While, the longitudinal fiber-dominated properties are not affected for the exposure durations investigated, it has been noted that extensive matrix erosion would ultimately limit effective load transfer to the reinforcing fibers and lead to the deterioration of mechanical properties even along the fiber dominated material direction.

**KEY WORDS:** carbon fiber-reinforced epoxy, environmental degradation, ultraviolet radiation, condensation, mechanical properties, tensile strength.

## INTRODUCTION

CARBON FIBER-REINFORCED EPOXY composites exhibit high specific strength, high specific stiffness and good fatigue tolerance, which have led to numerous advanced applications ranging from military and civil aircraft structures to recreational consumer products. Furthermore, the fabrication of components and structures from composites allows for the integration of design principles and manufacturing processes, resulting in optimally tailored mechanical and physical characteristics. Despite these inherent advantages, there are concerns regarding the overall long-term durability of these materials, especially as related to their capacity for sustained performance under harsh and changing environmental conditions. As a result, several investigations have focused on the

---

\*Author to whom correspondence should be addressed. E-mail: raman.singh@sunysb.edu

performance of fiber-reinforced composites when exposed to moisture, temperature, ultraviolet (UV) radiation, thermal cycling and mechanical fatigue [1]. However, the resulting degradation mechanisms are quite complex and usually dependent on the testing configuration and the specific material being investigated. This requires extensive experimental characterization of fundamental degradation mechanisms prior to the development of generalized models for predicting material behavior and long-term reliability. Furthermore, composite materials are typically exposed to multiple environments during service, which leads to the possibility of synergistic degradation mechanisms. Nevertheless, few investigations focus on the controlled determination of synergistic mechanisms. For example, combined exposure to UV radiation and water vapor, which are predominantly responsible for degradation during outdoor service, has received only limited attention [2–4]. In light of these issues, this investigation is focused on characterizing the physical, chemical and mechanical degradation of an advanced carbon fiber-reinforced epoxy composite following exposure to UV radiation and/or moisture (in the form of condensation). The objective is to explore the fundamental modes of degradation, establish synergistic mechanisms and thus provide a fundamental basis for predictive modeling of structural durability under these conditions.

Both UV radiation and moisture have adverse effects on the mechanical properties of the polymeric epoxy matrix, while the carbon fibers are not affected significantly by either environment. The polymer matrix in a fiber-reinforced composite serves to transfer applied loads to the reinforcing fibers and provide interlaminar shear strength, whereas the fiber–matrix interface governs the load transfer characteristics and damage tolerance. Thus, both these components represent weak links in fiber-reinforced composites and upon degradation, lead to reduced damage tolerance, and thus, lack of long-term durability.

The UV components of solar radiation incident on the earth surface are in the 290–400 nm band. The energy of these UV photons is comparable to the dissociation energies of polymer covalent bonds, which are typically 290–460 kJ/mole. Thus, UV photons absorbed by polymers result in photo-oxidative reactions that alter the chemical structure resulting in material deterioration [5]. These chemical reactions typically cause molecular chain scission and/or chain crosslinking. Chain scission lowers the molecular weight of the polymer, giving rise to reduced strength and heat resistance. On the other end, chain crosslinking leads to excessive brittleness and can result in microcracking. Photo-oxidative reactions can also result in the production of chromophoric chemical species, which may impart a discoloration to the polymer, if they absorb visible wavelengths. Furthermore, an autocatalytic degradation process is established if UV-absorbing chromophores are produced. Often, the formation of these groups serves as a convenient means of monitoring the deterioration process. Various photostabilizers may be added to polymers to slow down degradation by UV radiation. However, long-term exposure to UV radiation can still result in significant deterioration of mechanical properties, especially under conditions involving high ambient temperatures.

In contrast with the coatings literature, there are far few investigations that focus on the effects of UV radiation on the degradation of mechanical properties of fiber-reinforced polymer matrix composites [3,6–10]. For relatively short periods of exposure, only changes in surface morphology are observed [3,7]. However, for extended exposure to UV radiation, matrix dominated properties can suffer severe deterioration, e.g. interlaminar shear strength and flexural strength and flexural stiffness can all decrease [6,9,10]. The fiber-dominated properties, such as tensile modulus and tensile strength, are usually not affected significantly, especially for carbon fiber-reinforced materials [3,9].

The deteriorating effects of moisture on a polymeric matrix are not as severe as degradation by UV radiation. Moisture diffusion into the epoxy matrix leads to changes in thermophysical, mechanical, and chemical characteristics [11–13]. The epoxy can undergo plasticization and hydrolysis, which cause reversible and irreversible changes in the polymer structure. Due to these processes both the modulus and glass transition temperature are lowered [12–17]. Furthermore, matrix-dominated properties such as compressive strength, interlaminar shear strength, fatigue and impact tolerance can also deteriorate [12,15,16,18,19]. Plasticization is usually reversible upon desorption of moisture, while hydrolysis of chemical bonds results in permanent irreversible damage. At the same time, moisture wicking along the fiber–matrix interface can degrade the fiber–matrix bond, resulting in loss of microstructural integrity. Unlike glass and aramid fiber, carbon fibers themselves do not absorb moisture and their physical properties remain unaffected. However, as stated earlier, the deterioration of the matrix alone is sufficient to cause a decrease in performance and overall reliability.

Besides the degradation mechanisms discussed above, UV radiation and moisture can act in conjunction to further enhance the degradation of carbon fiber-reinforced epoxy composites. Microcracks which develop on a UV-irradiated surface provide pathways for rapid ingress of moisture and chemical agents. Moreover, the presence of moisture may enhance photo-oxidation reactions resulting in chain scission and/or chain crosslinking. Water vapor, especially in the form of condensation, can also remove soluble products of photo-oxidation reactions from a UV-irradiated surface and thereby expose fresh surfaces susceptible to further degradation by UV radiation. The combined effects of UV radiation and moisture have received only limited attention [2,3]. Few studies satisfactorily attempt to relate chemical and physical degradation mechanisms to changes in material properties and thereby predict durability and service life.

## EXPERIMENTAL DETAILS

A carbon fiber-reinforced epoxy composite was subjected to various UV radiation and/or condensation conditions. Physical degradation mechanisms resulting from different environmental exposures were monitored by weight loss and/or gain, and by micrographic observations of the composite surface. In addition, the degradation chemistry was examined using Fourier transform infrared spectroscopy (FTIR). Finally, the deterioration of mechanical properties was quantified by conducting uniaxial tension tests on various specimens that had been subjected to environmental degradation.

### Material Specification and Specimen Preparation

Specimens were machined from commercially fabricated  $[0]_8$ ,  $[90]_8$  and  $[0/90]_{2S}$  laminates of IM7/997 carbon-fiber–epoxy composite, which were donated by Cytec Engineered Materials (Anaheim, California). IM7 is a 5  $\mu\text{m}$  diameter, Polyacrylonitrile (PAN) based carbon fiber, while 997 is a 177°C (350°F) curing, thermoplastic modified, toughened epoxy resin with a proprietary formulation. The IM7/997 material system is currently under development and qualification for application to aerospace and rotorcraft structures. It is expected to provide higher damage tolerance than currently qualified materials such as IM7/5271-1 [20]. Typical properties of the IM7 fibers and the 997 epoxy

are listed in Table 1. The fiber volume fraction for all the three laminates was determined to be 58% based on image analysis of polished cross-sections.

Several specimens were machined using a water-cooled, high-speed diamond saw from each of the three  $[0]_8$ ,  $[90]_8$  and  $[0/90]_{2S}$  laminates, with nominal dimensions of  $152.4 \times 12.7 \times 1.27$  mm, as shown in Figure 1. Then the specimen edges were polished using 120, 400 and 600 grit paper to remove any microstructural damage induced during the machining process. The machined specimens were preconditioned in a desiccator at ambient temperature and 10% relative humidity for one to two weeks. The specimen's weight and dimensions were recorded just prior to the start of the environmental exposure cycle.

### Environmental Exposure Conditions

In order to study degradation mechanisms resulting from UV radiation and water condensation, the specimens were subjected to various exposure conditions in a QUV/Se weathering chamber (Q-Panel Lab Products, Cleveland, Ohio). The QUV/Se reproduces damage caused by sunlight, rain and dew by exposing materials to automated cycles of UV radiation and water vapor condensation. UV radiation is generated by eight fluorescent UV lamps that provide an excellent simulation of the UV component of solar radiation in the 295–365 nm region. The intensity of UV radiation is continuously monitored and controlled by four 'Solar-Eye' irradiance detectors. The detectors are calibrated every 400 h of service, and the lamps are replaced when they can no longer provide the required intensity. Water condensation is provided by the generation of vapor from a water bath.

**Table 1. Properties of IM7 carbon fiber and 997 epoxy.**

Property	IM7 Fiber	997 Epoxy
Longitudinal modulus (GPa)	276	4.14
Transverse modulus (GPa)	~20	4.14
Tensile strength (MPa)	5150	~90
Density (kg/m <sup>3</sup> )	1780	1310
Glass transition temperature (°C)	N/A	210

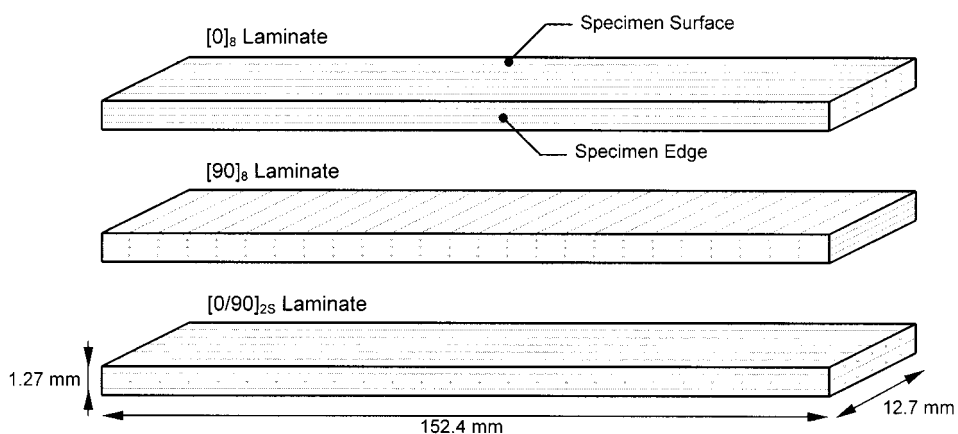


**Figure 1.** Schematic representation of the three different specimen configurations employed for investigation of degradation by UV radiation and/or condensation.

This vapor condenses on the specimen surface and thereby simulates rain and dew. Finally, the temperature inside the testing chamber can be elevated to provide accelerated degradation.

Several specimens of each of the three configurations,  $[0]_8$ ,  $[90]_8$  and  $[0/90]_{2S}$ , were subjected to the four different exposure conditions detailed below.

- A. *Exposure to Only UV Radiation* For this case, specimens were exposed to UV radiation in the 295–365 nm band at a temperature of 60°C. An irradiance level of 0.68 W/m<sup>2</sup> at 340 nm was chosen to match the typical maximum irradiance of summer sunlight at noon. The elevated temperature, selected to accelerate the degradation process, was small as compared to the glass transition temperature of epoxy ( $T_g \sim 210^\circ\text{C}$ ). Thus, it can be safely assumed that the degradation mechanisms themselves would not be affected.
- B. *Exposure to Only Condensation* In this exposure condition, the specimens were exposed to water vapor condensation at 50°C. Condensation on the specimen surface was achieved by water evaporation and resulted in 100% relative humidity inside the testing chamber. This condition simulates dew and rainfall, and results in both cyclic washing away of the specimen surface and in moisture absorption by Fickian diffusion through the epoxy matrix. As for the case of UV radiation exposure, the temperature was elevated slightly to accelerate the degradation process but not affect the basic mechanisms.
- C. *Sequential Exposure to UV Radiation followed by Condensation* In this exposure condition, the specimens were first exposed to only UV radiation followed by exposure to only condensation. The conditions for either exposure were the same as for the two independent exposure tests discussed above.
- D. *Cyclic Exposure to both UV Radiation and Condensation* In the final exposure condition, the specimens were exposed to alternating cycles consisting of 6 h of UV radiation followed by 6 h of condensation, the exposure conditions being the same as for single environment tests, as outlined above for exposure conditions A and B. The QUV/Se exposure chamber required  $\sim 20$  min to achieve thermal equilibrium when switching from one exposure condition to the next, which represented only five percent of the total exposure duration for a given condition.

The weight for each specimen was monitored during the entire duration of each environmental exposure test at time intervals of 24 h. For this purpose, the specimens were removed from the QUV/Se chamber, patted dry to remove any surface condensation and subsequently weighed in a high precision analytical balance. The specimens were then turned over and randomly repositioned in the exposure chamber to ensure uniform exposure on all surfaces. The total time required for monitoring specimen weight was approximately 10 min, which represented a minimal interruption in the exposure cycle.

Exposure conditions A and B were selected to investigate the independent effects of UV radiation and condensation, while conditions C and D were selected to investigate possible synergistic effects of the two environments. Exposure durations for each of the four environmental conditions are listed in Table 2. Note that, the exposure durations represent the time that each surface of the specimen is subjected to a given environment. Since the QUV/Se exposed only one of the two surfaces of the specimen at a given time and the specimens are turned over every 24 h, the equivalent exposure duration is actually half the total test duration. At the end of each exposure period, 250/500 h for A and B, and 500/1000 h for C and D, batches of specimens were removed from the environmental chamber for physical, chemical and mechanical characterization.

**Table 2. Duration of exposure for the four different environmental testing conditions.**

Environmental Condition	Equivalent Exposure Duration
UV radiation only	250 and 500 h
Condensation only	250 and 500 h
Sequential exposure	250 h of UV followed by 250 h of condensation 500 h of UV followed by 500 h of condensation
Cyclic exposure	500 h of combined UV and condensation (6 h cycle) 1000 h of combined UV and condensation (6 h cycle)

## DEGRADATION MECHANISMS

### Specimen Weight as Function of Exposure Duration

Figure 2 plots the variation of specimen weight as a function of time, for IM7/997 carbon fiber-reinforced epoxy exposed to only UV radiation (condition-A). Each curve represents averaged measurements obtained from four specimens. A rapid decrease in specimen weight occurred during the first 150 h of exposure, after which no appreciable changes were observed. This trend was exhibited by specimens for all three  $[0]_8$ ,  $[90]_8$  and  $[0/90]_{2S}$  laminates, with only minor differences in actual loss of weight. All specimens lost an average of 0.27% by weight after 500 h of exposure. This decrease in specimen weight is attributed to the expulsion of volatiles and residual moisture, which occurred early during exposure to UV radiation at 60°C.

On the other hand, specimens subjected to only water vapor condensation (condition-B) gained weight as a function of time, as shown in Figure 3. As for the previous case, each curve represents an averaged value determined from measurements for four specimens. The increase in specimen weight was due to absorption of water by the epoxy matrix and the weight-gain curves represent typical time-dependent Fickian diffusion. The specimens gained about 0.89% by weight, and were approaching complete saturation after 500 h of exposure to water vapor condensation at 50°C. Once again, trend was exhibited by specimens for all three  $[0]_8$ ,  $[90]_8$  and  $[0/90]_{2S}$  laminates, with only minor differences in actual weight gain.

When the composite specimens were subjected to sequential exposure by UV radiation followed by condensation (condition-C), the results were as expected from the observations made for individual exposure conditions. As shown in Figure 4, the specimens initially lost weight during the UV radiation cycle and subsequently gained weight during the condensation cycle. This behavior was in accordance with the weight changes observed during exposure to either only UV radiation, or only condensation, and the actual change in weight was a simple time-shifted linear superposition of results obtained for individual exposure conditions. However, when the specimens were cyclically exposed to both UV radiation and condensation (condition-D) the change in specimen weight was completely unexpected, as shown in Figure 5. A simple superposition of observations carried out for single environmental exposure conditions would predict an increase in specimen weight as a function of exposure duration. In contrast, the specimens started to exhibit a decrease in weight after about 125 h of exposure. This weight loss continued at a steady rate for the remainder of the test. An average of 1.25% decrease in specimen weight was observed after 1000 h of cyclic exposure to UV radiation and

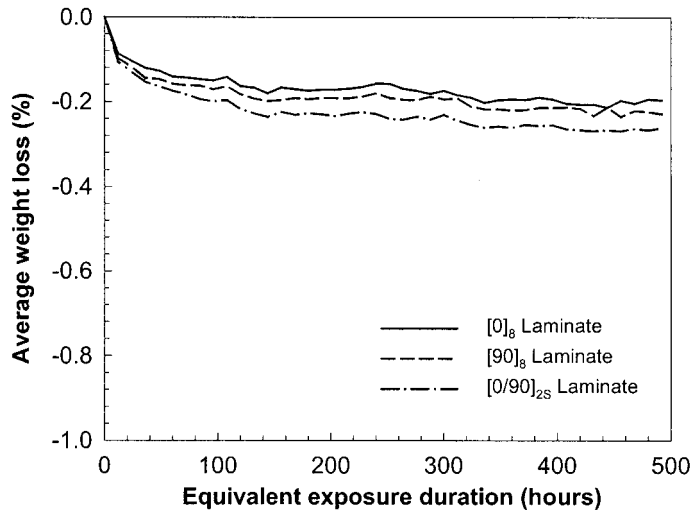


Figure 2. Change in specimen weight, as a function of time, for exposure to only UV radiation.

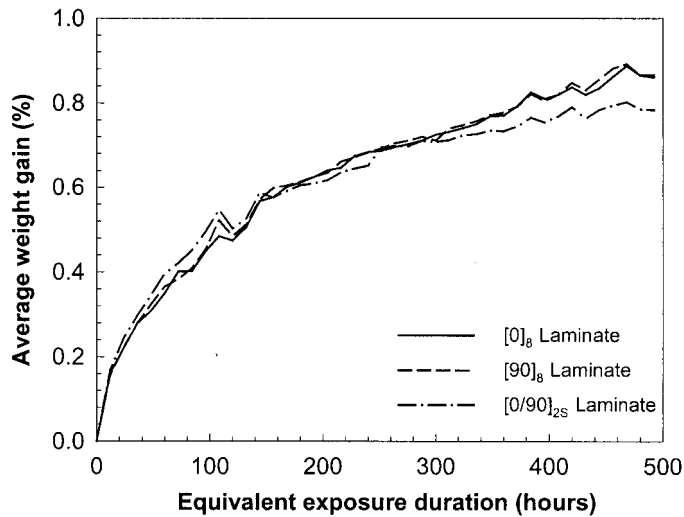
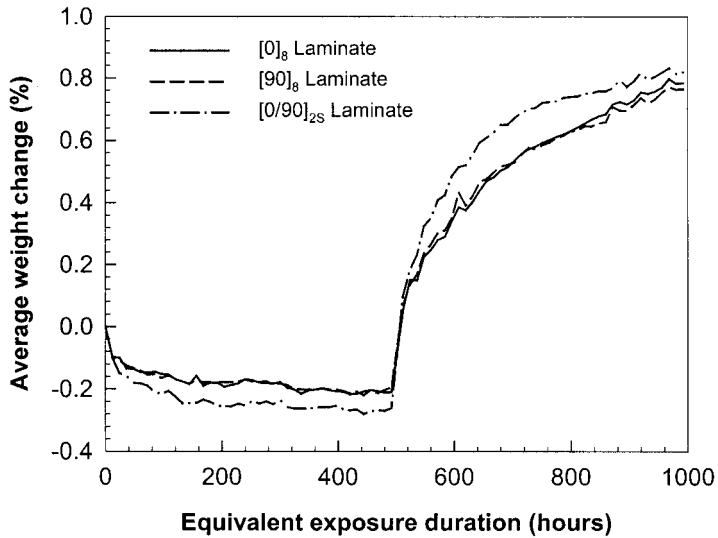


Figure 3. Change in specimen weight, as a function of time, for exposure to only condensation.

condensation. Moreover, the specimen weight was still decreasing steadily at the end of the test duration, which suggests that the weight loss would have continued further with more exposure to UV radiation and condensation. The greatly enhanced loss of specimen weight under cyclic exposure indicated that material was being removed from the composite specimens. This was confirmed by optical microscopy as discussed in the following section.

### Surface Morphology

Surfaces of all specimens exposed to UV radiation exhibited a distinct change in color from black to dark green during early stages of the exposure duration. The discoloration



**Figure 4.** Change in specimen weight, as a function of time, for sequential exposure to UV radiation followed by condensation.

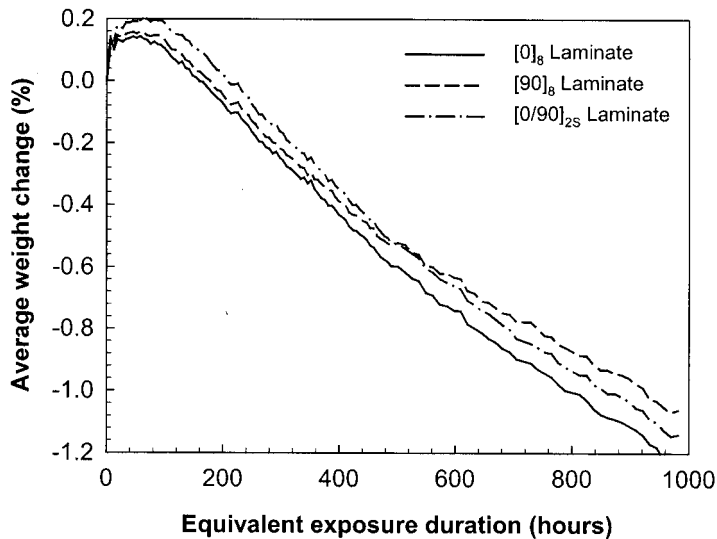
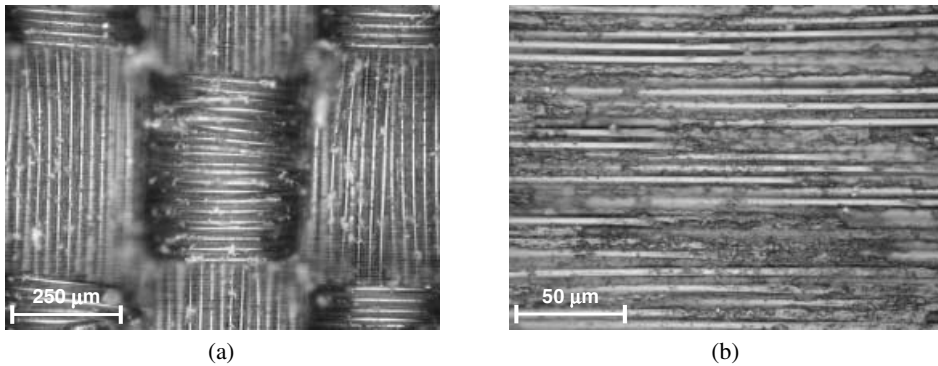


**Figure 5.** Change in specimen weight, as a function of time, for cyclic exposure to both UV radiation and condensation.

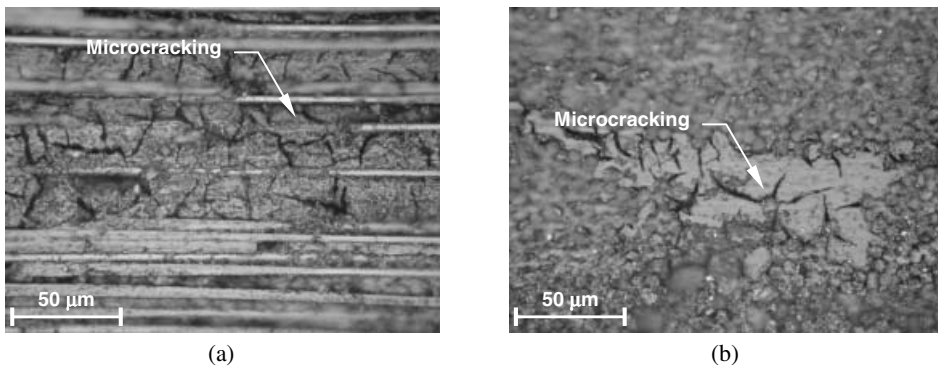
established that photo-oxidation resulted in the formation of chromophoric chemical species, which absorbed in the visible range of light. Minor changes in surface roughness were also visible by the naked eye for all specimens exposed to UV radiation. Exposure to water vapor condensation did not result in any visible changes in specimen morphology. Further details regarding the physical processes that govern material degradation were revealed by examination of the specimens under an optical microscope. Both specimen surfaces and edges were examined for all the three  $[0]_8$ ,  $[90]_8$  and  $[0/90]_{2S}$  configurations.

Figure 6 shows optical micrographs of the machined specimens before being subjected to any environmental exposure. The specimen surface was characterized by a ‘weave pattern’, as shown in Figure 6(a). This represents an epoxy rich layer, and is actually the impression left by the peel-ply fabric used during the laminate fabrication process. No surface damage was observed in any of the laminates, either due to the fabrication process or due to machining, as shown in Figure 6(b).

No changes in morphology were observed at low magnifications for either the specimen surface or edge, for specimens exposed to 500 h of UV radiation. However, higher magnification images, shown in Figures 7(a) and (b), revealed the formation of microcracks in the epoxy matrix. This phenomenon was caused by the polymer matrix becoming excessively brittle due to increased crosslinking resulting from photo-oxidation reactions induced by UV radiation. In contrast, exposure of the composite specimens to 500 h of water vapor condensation did not result in any significant changes in morphology, as illustrated in Figure 8. The specimen surfaces and edges generally appeared to be identical to those observed prior to environmental exposure, and only minor differences were noted at high magnification observations of the edges of  $[90]_8$  specimens, as shown in Figure 8(b). In this case, the carbon fibers were more clearly demarcated within the epoxy matrix and the latter exhibited some expansion ostensibly



**Figure 6.** Optical micrographs for composite specimen prior to environmental exposure: (a) surface of  $[0]_8$  specimen; (b) edge of a  $[0]_8$  specimen at high magnification.



**Figure 7.** Optical micrographs after 500 h of exposure to UV radiation: (a) edge of a  $[0]_8$  specimen at high magnification; (b) edge of a  $[90]_8$  specimen at high magnification.

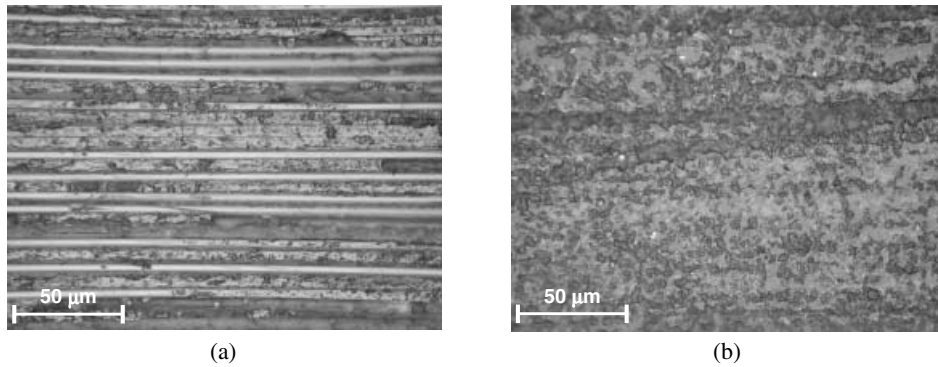


**Figure 8.** Optical micrographs after 500 h of exposure to condensation: (a) edge of a  $[0]_8$  specimen at high magnification; (b) edge of a  $[90]_8$  specimen at high magnification.

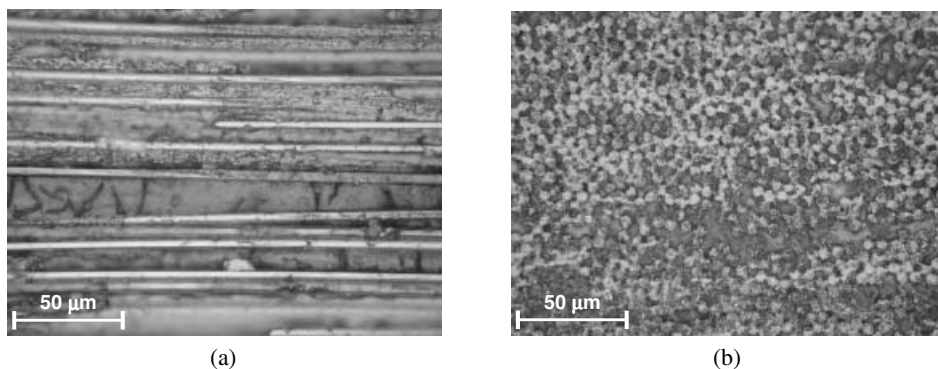


**Figure 9.** Optical micrographs after sequential exposure to 500 h of UV radiation followed by 500 h of condensation: (a) edge of a  $[0]_8$  specimen; (b) edge of a  $[90]_8$  specimen.

due to moisture-induced strains. The fiber–matrix interface was not affected in either case of exposure to only UV radiation or only condensation. Specimens exposed sequentially to UV radiation followed by condensation exhibited surface characteristics that were essentially a combination of the two individual exposure conditions. The top surface of the specimen did not show appreciable degradation and the ‘weave pattern’ was still visible. However, the epoxy matrix exhibited limited microcracking and erosion, as illustrated in Figures 9(a) and (b).

Cyclic exposure to both UV radiation and condensation resulted in physical degradation that was very different from all the other environmental exposure conditions. Figure 10 shows a series of images for specimens exposed to 1000 h of combined UV radiation and condensation on a 6 h repeat cycle. In all cases, both the specimen surfaces and edges exhibited severe physical degradation in the form of extensive matrix erosion, void formation and fiber–matrix interface debonding. As shown in Figure 10(a), the epoxy rich layer on the specimen surface was completely removed and the underlying carbon fibers were exposed. Erosion of the epoxy matrix also resulted in fiber loss and extensive microcracking. Figure 10(b) reveals a region on the edge of a  $[0]_8$  specimen which exhibited fiber loss and thus exposed the underlying matrix. Fiber loss was also established from the

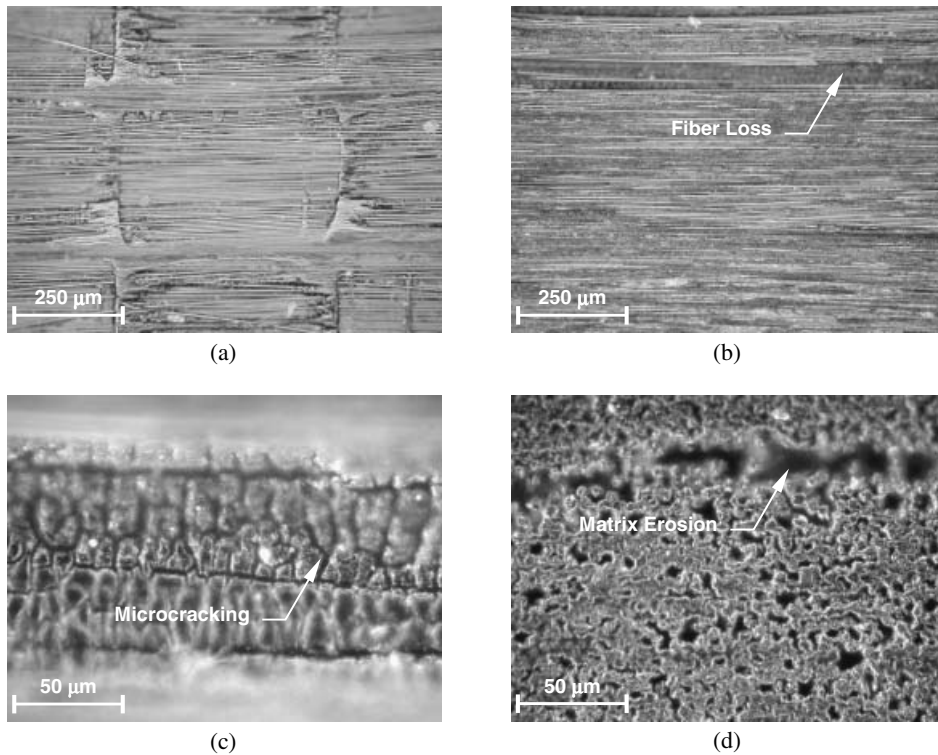


**Figure 10.** Optical micrographs after 1000 h of cyclic exposure to both UV radiation and condensation: (a) surface of a  $[0]_8$  specimen; (b) edge of a  $[0]_8$  specimen; (c) edge of a  $[0]_8$  specimen at higher magnification; (d) edge of a  $[90]_8$  specimen at higher magnification.

presence of fiber residue in the runoff water collected during the experiment. Figure 10(c) shows details of extensive microcracking in the epoxy matrix. For the case of  $[90]_8$  specimens, epoxy erosion resulted in extensive voiding, as shown in Figure 10(d). The matrix removal process also resulted in a 7.5% decrease in average specimen thickness. Matrix erosion was the result of synergistic degradation mechanisms. Exposure to UV radiation results in the formation of a thin surface layer of chemically modified epoxy. Subsequent water condensation leaches away soluble degradation products, which exposes a fresh layer that can once again be attacked by UV radiation. In this manner, a repetitive process is established that leads to significant erosion of the epoxy matrix. Furthermore, it is also conceivable that the presence of absorbed water molecules in the epoxy matrix can enhance the photo-oxidation reactions due to increased availability of  $\text{OH}^-$  and  $\text{H}^+$  ions. This matrix erosion process would have continued even after the 1000 h exposure duration employed in these experiments, as evidenced by the decreasing weight loss curve shown in Figure 5. The matrix erosion process has a significantly adverse effect on the integrity of the epoxy-rich inter-ply region in composite laminates. This is illustrated by a direct comparison of the images of  $[0/90]_{2S}$  cross-ply specimens exposed to various environments, as shown in Figure 11. This series of images demonstrates that severe erosion of the epoxy matrix due to synergistic effects of UV radiation and condensation will lead to loss of structural integrity in laminated composite structures.

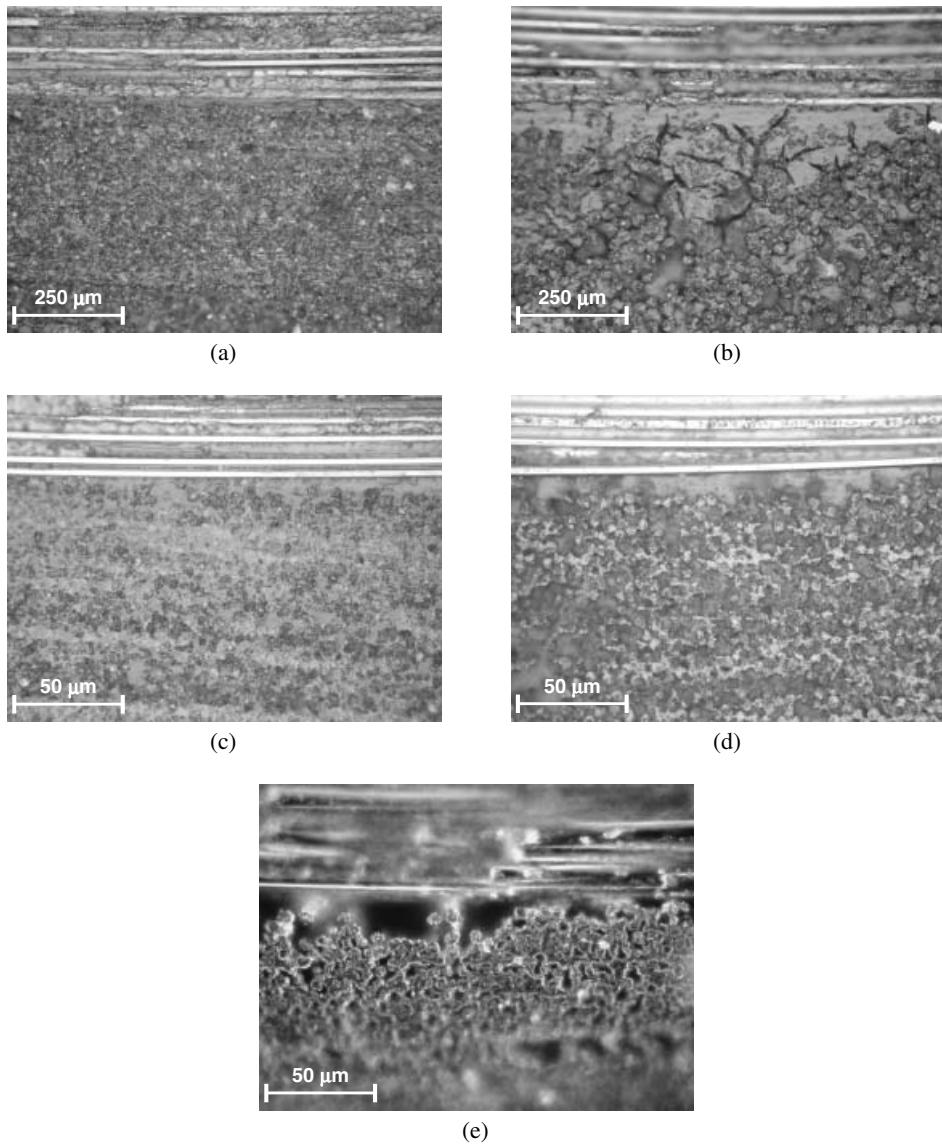


**Figure 11.** Optical micrographs for the edge of  $[0/90]_{2S}$  specimens exposed to various environments: (a) undegraded; (b) exposed to only UV radiation; (c) exposed to only condensation; (d) sequentially exposed to UV radiation followed by condensation; (e) cyclically exposed to UV radiation and condensation.

### Chemical Changes due to Environmental Exposure

Environmentally degraded composite specimens were analyzed using FTIR spectroscopy to determine the effects of UV radiation and condensation on the surface chemistry. The specimen surfaces were imaged using an infrared microscope equipped with a  $15\times$  diffuse reflectance objective and the FTIR spectra were determined by a Nicolet 560 spectrometer that provided a  $2\text{ cm}^{-1}$  resolution.

The spectra did not exhibit appreciable changes, upon specimen exposure to either UV radiation or condensation, for the 1700–4000  $\text{cm}^{-1}$  region. This region was primarily characterized by a broad peak at 3399  $\text{cm}^{-1}$  representing the OH group. However, certain differences were observed for the 900–1700  $\text{cm}^{-1}$  region. Figure 12 plots the FTIR spectra for specimens that were undegraded, exposed to 500 h of only UV radiation and exposed to 500 h of only condensation. The spectrum obtained for specimens exposed to only condensation had similar characteristics as that of an undegraded specimen. However, various changes were observed for specimens that were subjected to only UV radiation. There were reductions in the peaks at 1250 and 1509  $\text{cm}^{-1}$ . These two peaks were attributed to oxirane ring stretching vibrations of the epoxy, and to N–H deformation of polyamine cross-linker, respectively [21]. The reduction of both these peaks indicated the absorbance of atmospheric oxygen and suggested an increase in the cross-link density of the epoxy [21,22]. This increased crosslinking leads to excessive brittleness and can result in microcracking. Note that the presence of these peaks indicates that the composites were under-cured and that further curing took place during the environment testing. A reduction in the peak at 1296  $\text{cm}^{-1}$  was also observed, and was attributed to C–N stretching vibrations due to amide formation. This observation indicated the presence of chain scission reactions.

Previous studies on the UV degradation of epoxies have showed that both crosslinking and chain scission mechanisms operate in a competing manner during the degradation process. Increased crosslinking dominates in the early stages of degradation, after which carbonyl amide formation by chain scission takes over [21]. Both these mechanisms then result in increased microcracking and surface deterioration, and exact chemical degradation reactions can be established on the basis of the epoxy chemistry. In the present case, further analysis was not possible other than the general observations made

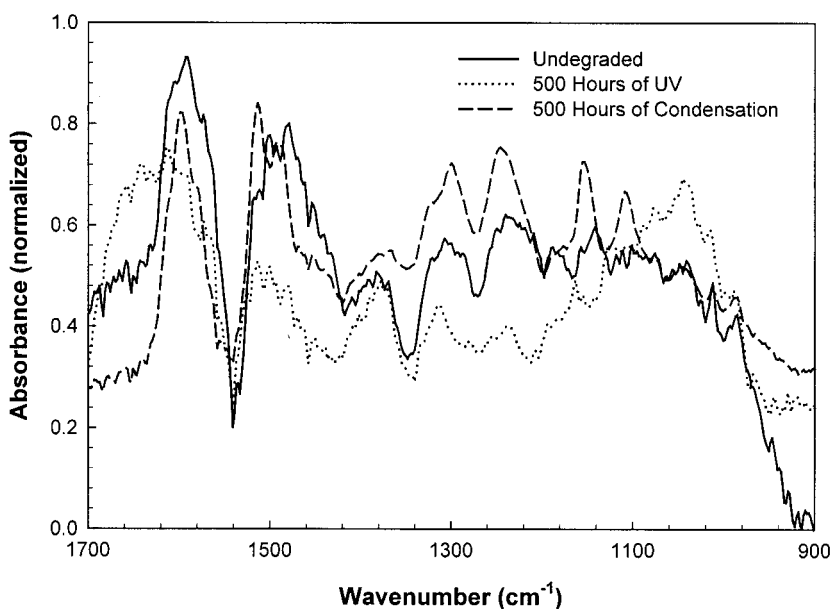


**Figure 12.** FTIR spectra for IM7/997 specimens that were undegraded, exposed to 500 h of only UV radiation and exposed to 500 h of only condensation.

above. This was due to the lack of information regarding the exact chemical nature of the 997 epoxy, which has a proprietary formulation.

## MECHANICAL PROPERTIES

### Testing Methodology

Uniaxial tension testing was conducted to determine the effects of degradation by UV radiation and condensation on the deterioration of mechanical properties. Various specimen configurations were tested to determine the longitudinal and transverse moduli,  $E_L$  and  $E_T$ , the Poisson's ratio,  $\nu_{LT}$ , the ultimate longitudinal tensile strength,  $F_L^u$ , and the transverse tensile strength,  $F_T^u$ . Since the objective was to determine irreversible degradation in properties, the specimens were held in a desiccator for one week prior to tensile testing.

The specimen surface was cleaned using acetone, and a 350 $\Omega$ , two-element, 90° tee rosette strain gage (CEA-06-125UT-350, Vishay Measurements Group, Raleigh, North Carolina) was mounted on the center of the specimen using a room-temperature curing adhesive. The strain gage resistance and grid-area were selected especially for use with composite materials. Also, the use of a room-temperature curing adhesive ensured that no changes in composite properties would occur during the strain gage bonding process. The specimens were then subjected to uniaxial loading in tension on a servo-hydraulic universal testing machine in displacement-controlled mode with crosshead displacement rate of 0.381 mm/min. The ends of the specimens were untabbed and held in wedge grips with 100-grit sandpaper. The use of untabbed geometries is as per current recommendations for testing of composite materials [23–25]. During the testing process, the longitudinal and transverse strains, and the applied load were recorded on a digital storage oscilloscope. A typical stress–strain plot obtained for a  $[0/90]_{2S}$  specimen is shown in Figure 13.

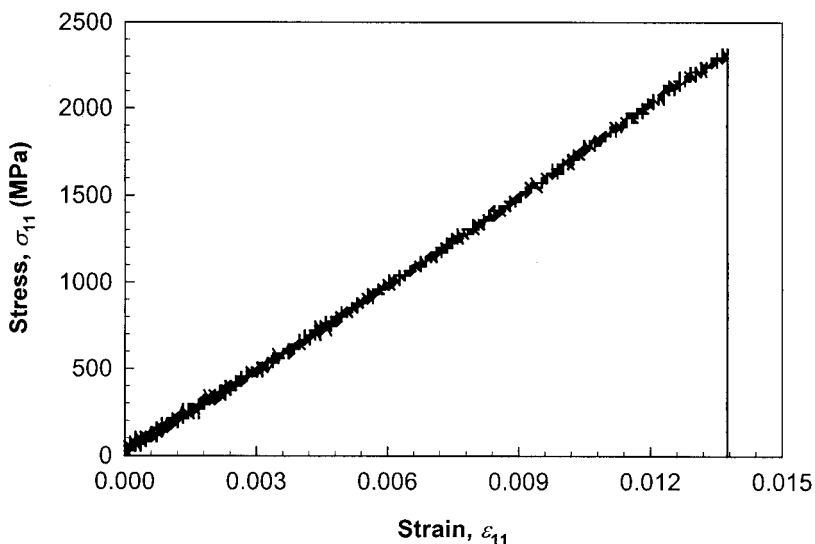


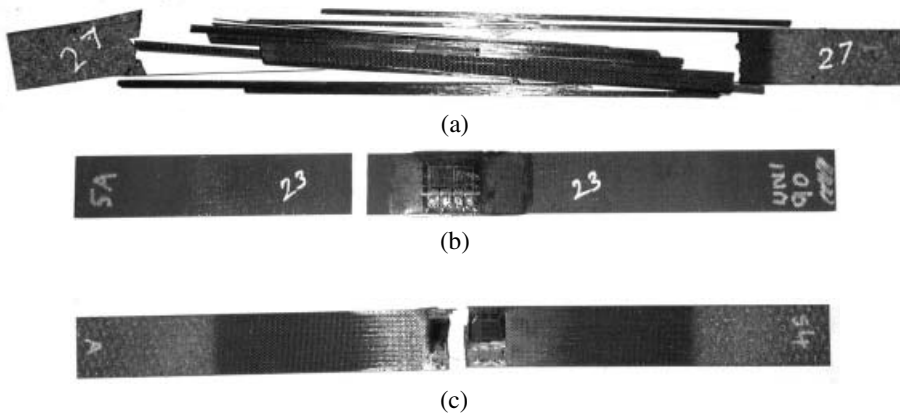
Figure 13. A typical stress–strain plot for uniaxial tension testing of a  $[0/90]_{2S}$  specimen.

Table 3 lists the use of specific specimen configurations for determining the various mechanical properties of interest. Longitudinal elastic properties,  $E_L$  and  $\nu_{LT}$ , were determined from tests conducted on  $[0]_8$  specimens, while transverse elastic properties,  $E_T$  and  $\nu_{TL}$ , were determined from  $[90]_8$  specimens. For appropriate determination of the ultimate longitudinal and transverse tensile strengths,  $F_L^{ut}$  and  $F_T^{ut}$ , it is required that the specimens fail by a valid mode of failure. Figure 14(a) illustrates the failure modes for the three specimen configurations. The unidirectional  $[0]_8$  specimens failed by axial splitting, the  $[90]_8$  specimens failed by transverse matrix failure, and the  $[0/90]_{2S}$  specimens failed by fiber breakage. Failure by axial splitting results from lack of transverse constraint and does not represent a valid failure mode for the determination of fiber-dominated longitudinal tensile strength. Thus, it was not appropriate to relate the failure load obtained for the  $[0]_8$  specimens to the longitudinal tensile strength,  $F_L^{ut}$ . On the other hand,  $[0/90]_{2S}$  cross-ply specimens failed by fiber breakage, which represents a valid failure mode for fiber-dominated properties. Thus, the uniaxial tensile strength of the cross-ply specimens,  $F^{ut}$ , was used to determine the longitudinal tensile strength,  $F_L^{ut}$ , as per Equation (1) [23,24],

$$F_L^{ut} = F^{ut} \frac{E_L[(E_L + E_T)/2] - (\nu_{LT}E_T)^2}{[(E_L + E_T)/2]^2 - (\nu_{LT}E_T)^2} \tag{1}$$

**Table 3. Determination of elastic properties and tensile strength from specimens of various configurations.**

Material Property	Specimen Configuration
Longitudinal elastic properties, $E_L$ and $\nu_{LT}$	$[0]_8$
Transverse elastic properties, $E_T$ and $\nu_{TL}$	$[90]_8$
Longitudinal tensile strength, $F_L^{ut}$	$[0/90]_{2S}$ , $[0]_8$ , and $[90]_8$
Transverse tensile strengths, $F_T^{ut}$	$[90]_8$



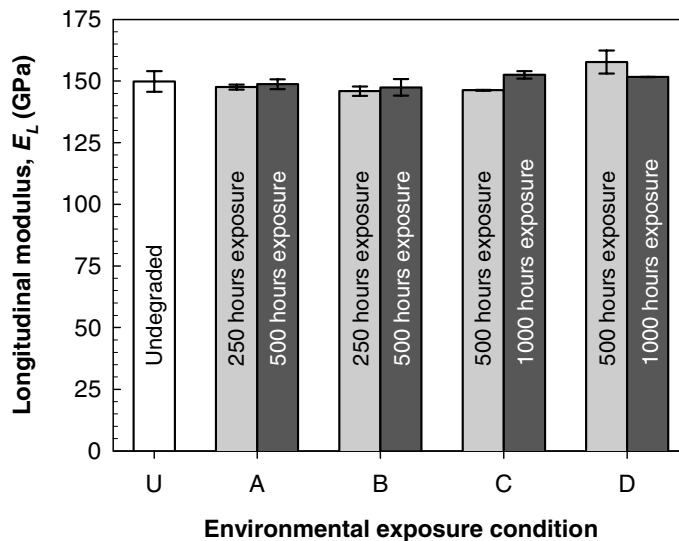
**Figure 14.** Failure modes under uniaxial tension: (a) axial splitting for  $[0]_8$  specimens, (b) transverse matrix failure for  $[90]_8$  specimens; (c) fiber breakage for  $[0/90]_{2S}$  specimens.

where,  $E_L$  is the longitudinal modulus,  $E_T$  is the transverse modulus, and  $\nu_{LT}$ , is the Poisson's ratio, which are all experimentally determined properties. Finally, it was possible to directly determine the transverse tensile strength,  $F_T^u$  based on the failure load observed for the  $[90]_8$  specimens.

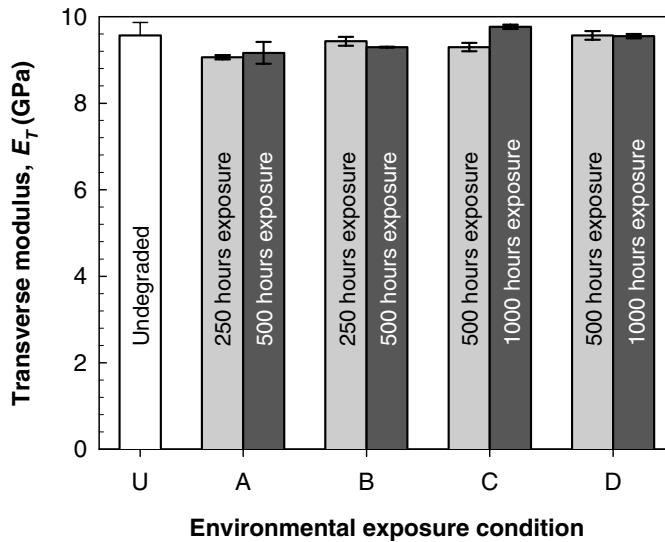
### Elastic Modulus and Poisson's Ratio

Figure 15 plots the variation of the longitudinal tensile modulus,  $E_L$ , for specimens exposed to various combinations of UV radiation and/or only condensation. This modulus was measured by uniaxial tensile tests on  $[0]_8$  specimens subjected to the different degradation conditions. Several tests were conducted for each degradation condition, and the error bars denote spread of experimental data. As shown in Figure 15, no appreciable change in  $E_L$  was observed for any of the exposure conditions A, B, C, or D. This result was as expected, since, neither UV radiation nor condensation lead to degradation of the carbon fiber. Thus, fiber dominated properties, such as  $E_L$ , are not expected to change.

A variation of the transverse modulus,  $E_T$ , is plotted in Figure 16 as a function of exposure to various combinations of UV radiation and/or only condensation. The modulus was measured by uniaxial tensile tests on  $[90]_8$  specimens. As before, several tests were conducted for each degradation condition to establish the spread of experimental data. A decrease of 4.2% in the transverse modulus,  $E_T$ , was observed for specimens exposed to 500 h only UV radiation. This decrease indicates that the molecular weight of the epoxy matrix was reduced due to chain-scission reactions induced by photo-oxidation from UV radiation. The small amount of actual decrease in the value of  $E_T$  is due to the fact that changes induced by UV radiation are a surface phenomena, while  $E_T$  represents a bulk material property. A small, but measurable, decrease of 2.8% in the transverse modulus was also observed for specimens exposed to 500 h of only condensation.



**Figure 15.** Variation of longitudinal modulus,  $E_L$ , for exposure to UV radiation and/or condensation: U – undegraded with no exposure, A – exposure to only UV radiation, B – exposure to only condensation, C – sequential exposure, and D – cyclic exposure.



**Figure 16.** Variation of transverse modulus,  $E_T$ , for exposure to UV radiation and/or condensation: U – undegraded with no exposure, A – exposure to only UV radiation, B – exposure to only condensation, C – sequential exposure, and D – cyclic exposure.

This decrease in  $E_T$  after exposure to condensation indicates that the epoxy matrix underwent hydrolysis and irreversible plasticization. However, no trend could be established for specimens exposed to both UV radiation and condensation, either sequentially or cyclically. The measured values of the transverse modulus,  $E_T$ , for either of these two exposure conditions, were the same as those for the undegraded specimens not exposed to any environment. This indicates that there are some synergistic effects that govern the changes in matrix properties when the specimens are exposed to a combination of both UV radiation and condensation.

Figure 17 shows the variation of the major Poisson's ratio,  $\nu_{LT}$ , for exposure to various conditions of UV radiation and/or condensation. These measurements were determined by recording both longitudinal and transverse strains during uniaxial tension tests carried out on  $[0]_8$  specimens. There was no appreciable change in the value of  $\nu_{LT}$  as a function of environmental exposure. The minor Poisson's ratio  $\nu_{TL}$  was also determined by recording longitudinal and transverse strains during uniaxial tension tests carried out on  $[90]_8$  specimens and no appreciable changes were observed.

### Ultimate Tensile Strength

Figure 18 plots the variation of the longitudinal tensile strength,  $F_L^u$ , for specimens exposed to various combinations of UV radiation and/or only condensation. The longitudinal tensile strength was determined from the ultimate failure load for  $[0/90]_{2S}$  specimens using Equation (1), as discussed earlier. Once again, several test were conducted for each degradation condition, and the error bars denote spread of experimental data. As shown in Figure 18, no appreciable changes in  $F_L^u$  were observed for any of the exposure conditions A, B, C, or D. The longitudinal tensile strength is a fiber-dominated property.

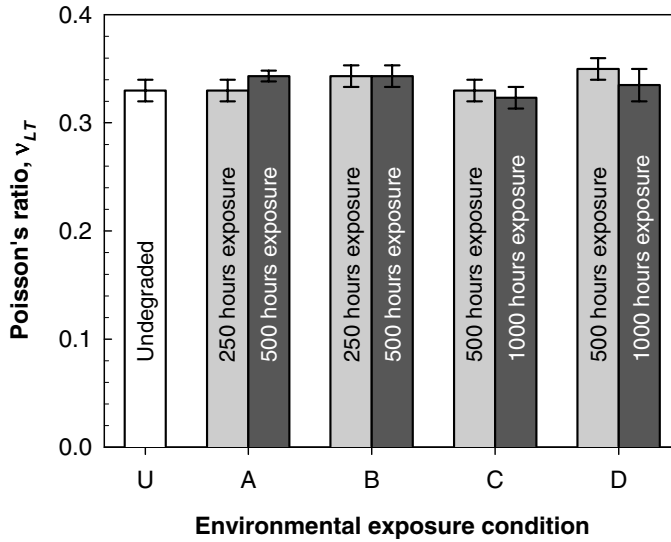


**Figure 17.** Variation of major Poisson's ratio,  $\nu_{LT}$ , for exposure to UV radiation and/or condensation: U – undegraded with no exposure, A – exposure to only UV radiation, B – exposure to only condensation, C – sequential exposure, and D – cyclic exposure.

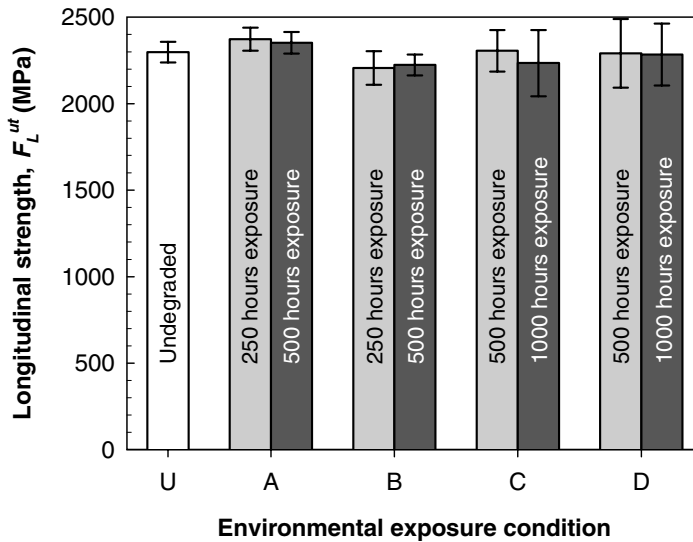


**Figure 18.** Variation of longitudinal tensile strength,  $F_L^{ut}$ , for exposure to UV radiation and/or condensation: U – undegraded with no exposure, A – exposure to only UV radiation, B – exposure to only condensation, C – sequential exposure, and D – cyclic exposure.

Since the carbon fibers themselves are not affected by either UV radiation or condensation,  $F_L^{ut}$  is not expected to change.

The degradation of the epoxy matrix resulted in significant deterioration of the transverse tensile strength,  $F_T^{ut}$ , as plotted in Figure 19. Specimens exposed to 500 h of only UV radiation exhibited a 9% decrease in the transverse tensile strength. This decrease

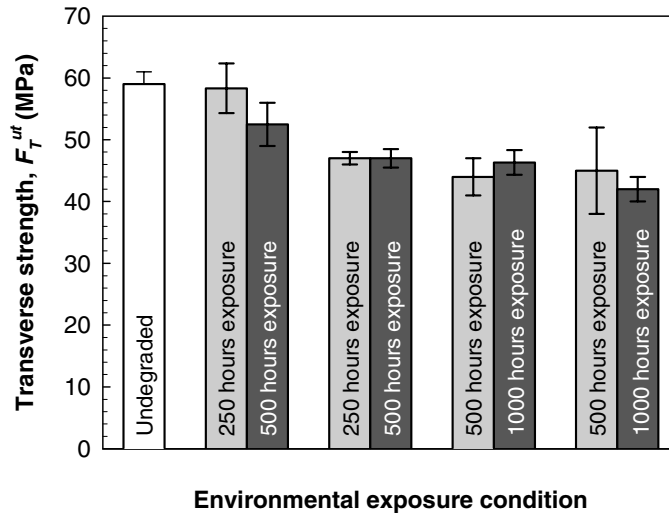


**Figure 19.** Variation of transverse tensile strength,  $F_T^{ut}$ , for exposure to UV radiation and/or condensation: U – undegraded with no exposure, A – exposure to only UV radiation, B – exposure to only condensation, C – sequential exposure, and D – cyclic exposure.

in strength was due to the presence of surface microcracks induced by exposure to UV radiation. A decrease of 20% in  $F_T^{ut}$  was observed when specimens were exposed to 500 h of only condensation, which was due to irreversible hydrolysis and plasticization of the epoxy matrix. Specimens exposed to sequential exposure of 1000 h of UV radiation followed by 1000 h of condensation exhibited a similar decrease of 21% in the transverse tensile strength. The degradation was most severe for specimens exposed to cyclic UV radiation and condensation. After 1000 h of cyclic exposure the transverse tensile strength was decreased by 29% as compared to undegraded specimens not exposed to any environment. This deterioration was in accordance with extensive matrix erosion observed for cyclic exposure and was quite severe considering that the specimens were exposed to a total duration of only 1000 h!

## CONCLUSION

An experimental investigation has been conducted to characterize the physical, chemical and mechanical degradation of an IM7/997 carbon fiber-reinforced epoxy composite following exposure to UV radiation and water vapor condensation. Specimens fabricated from  $[0]_8$ ,  $[90]_8$  and  $[0/90]_{2S}$  laminates were subjected to four different exposure environments of UV radiation (295–365 nm,  $0.68 \text{ W/m}^2$  irradiance at 340 nm,  $60^\circ\text{C}$  temperature) and/or condensation (100% relative humidity,  $50^\circ\text{C}$  temperature). Physical degradation mechanisms resulting from different environmental exposures were identified by monitoring weight loss and/or gain, and by micrographic observations of the composite surface. In addition, the degradation chemistry was examined using FTIR spectroscopy. The deterioration of mechanical properties was then quantified by conducting uniaxial tension tests on various specimen configurations subjected to environmental degradation.

Specimens exposed to 500 h of only UV radiation exhibited a minor 0.27% decrease in weight, which was attributed to the expulsion of volatiles and residual moisture. On the

other hand, specimens that were subjected to only water vapor condensation gained weight, and demonstrated a typical of time-dependent Fickian diffusion behavior. These specimens gained 0.89% by weight and approached complete saturation after 500 h of exposure to condensation. When specimens were exposed sequentially to UV radiation followed by condensation, the results were as expected from the observations made for individual exposure conditions. The specimens initially lost weight during the UV radiation cycle and subsequently gained weight during the condensation cycle, and the actual change in weight was a simple time-shifted linear superposition of results obtained for individual exposure conditions. However, when the specimens were cyclically exposed to both UV radiation and condensation, the change in specimen weight was completely unexpected. These specimens exhibited continuous weight loss at a steady rate throughout the exposure duration, which indicated that material was being removed from the composite specimens. Based on micrographic observations and FTIR analysis it was determined that UV radiation and condensation operate in a synergistic manner that leads to extensive matrix erosion, matrix microcracking, fiber debonding, fiber loss and void formation.

The effects of environmental degradation on mechanical properties were established by conducting a series of uniaxial tension tests to determine the elastic moduli and failure strengths in the longitudinal and transverse directions. It was determined that the matrix-dominated, transverse properties can undergo severe deterioration. Most significant changes were observed for the transverse tensile strength,  $F_T^{ut}$ . It was observed that only 1000 h of cyclic exposure to both UV radiation and condensation resulted in a 29% decrease in the transverse tensile strength of the material. The transverse modulus was also reduced, but not as severely as the transverse strength. The longitudinal fiber-dominated properties were not affected for the exposure durations employed in this investigation. However, it can be expected that over long periods of environmental exposure, the synergism between UV and condensation will cause so much damage that load transfer between fibers will longer possible owing to matrix erosion. This would then lead to deterioration of even fiber-dominated properties such as  $E_L$  and  $F_L^{ut}$ , and could even result in catastrophic structural failure.

### ACKNOWLEDGMENTS

We gratefully acknowledge the support of the US Army Research Office for supporting this research investigation (Grant No. DAAD19-00-1-0518). We are also thankful to Mr. Joe Morris and Mr. Sabah Fattohi (Cytac Engineered Materials, Anaheim, California) for donating IM7/997 composite laminates, and to Profs. C. R. Clayton and G. Halada (Department of Materials Science, SUNY Stony Brook) for assistance in carrying out the FTIR spectroscopy.

### REFERENCES

1. Springer, G.S. (ed.) (1984). *Environmental Effects on Composite Materials*, Vol. 1–3, Technomic Publishing Co., Inc., Lancaster, PA.
2. Blaga, A. and Yamasaki, R.S. (1973). *Journal of Materials Science*, **8**: 654–666.
3. Chin, J.W., Nguyen, T. and Aouadi, K. (1997). *Journal of Composites Technology and Research*, **19**: 205–213.

4. Chung, D.D.L. (1994). *Carbon Fiber Composites*, Butterworth-Heinemann, Boston, MA.
5. Ranby, B. and Rabek, J.F. (1975). *Photodegradation, Photo-Oxidation and Photostabilization of Polymers*, John Wiley and Sons, London.
6. Hancox, N.L. and Minty, D.C.C. (1977). *Journal of the British Interplanetary Society*, **30**: 391–399.
7. Phelps, H.R. and Long, E.R. Jr. (1980). *Journal of Composite Materials*, **14**: 334–341.
8. Giori, C. and Yamauchi, T. (1984). *Journal of Applied Polymer Science*, **29**: 237–249.
9. Liao, W.B. and Tseng, F.P. (1998). *Polymer Composites*, **19**: 440–445.
10. Shin, K.-B., Kim, C.-G., Hong, C.-S. and Lee, H.-H. (2000). *Composites, Part B-Engineering*, **31**: 223–235.
11. Shen, C.H. and Springer, G.S. (1976). *Journal Of Composite Materials*, **10**: 2–20.
12. Weitsman, Y.J. (1991). In: Reifsnider, K.L. (ed.), *Fatigue of Composite Materials*, pp. 385–429, Elsevier, New York.
13. Jones, F.R. (1999). In: Pritchard, (ed.), *Reinforced Plastics Durability*, pp. 70–110, Woodhead Publishing Company.
14. Zheng, Q. and Morgan, R.J. (1993). *Journal Of Composite Materials*, **27**: 1465–1478.
15. Adams, R.D. and Singh, M.M. (1996). *Composites Science and Technology*, **56**: 977–997.
16. Zhao, S.X. and Gaedke, M. (1996). *Advanced Composite Materials*, **5**: 291–307.
17. Choi, H.S., Ahn, K.J., Nam, J.D. and Chun, H.J. (2001). *Composites, Part A – Applied Science and Manufacturing*, **32**: 709–720.
18. Soutis, C. and Turkmen, D. (1997). *Journal Of Composite Materials*, **31**: 832–849.
19. Sala, G. (2000). *Composites, Part B – Engineering*, **31**: 357–373.
20. Morris, J. (2001). *Private Communication*, Cytec Engineered Materials, Anaheim, California.
21. Kim, H. and Urban, M.W. (2000). *Langmuir*, **16**: 5382–5390.
22. Hepburn, D.M., Kemp, I.J. and Cooper, J.M. (2000). *Polymer Degradation and Stability*, **70**: 245–251.
23. Rawlinson, R.A. (1991). In: *Proceedings of the 36th International SAMPE Symposium*, pp. 1058–1068.
24. Hart-Smith, L.J. (1991). In: *Proceedings of the 36th International SAMPE Symposium*, pp. 1029–1044.
25. ASTM D3039/D3039M-00. (2000). American Society for Testing and Materials. West Conshohocken, PA.